Petroleum 7 (2021) 209–221

Contents lists available at ScienceDirect

Petroleum

journal homepage: www.keaipublishing.com/en/journals/petlm

Numerical modeling of the critical pipeline inclination for the elimination of the water accumulation on the pipe floor in oil-water fluid flow

Xiaoqin Song [a], Dongxin Li [a, *], Xiao Sun [b], Xingjie Mou [c], Y. Frank Cheng [d], Yuexin Yang [e]

[a] State Key Laboratory of Oil and Gas Reservoir Geology and Exploitation, Southwest Petroleum University, Chengdu, 610500, China
[b] Petrochina Southwest Pipeline Company, Chengdu, 610500, China
[c] Downhole Operation Company, Sinopec Xinan Oilfield Service Corporation, Deyang, 618000, China
[d] Dept. of Mechanical Engineering, University of Calgary, Calgary, AB, T2N 1N4, Canada
[e] Civil Aviation Flight University of China, Guanghan, 618307, China

ARTICLE INFO

Article history:
Received 11 January 2020
Received in revised form
15 April 2020
Accepted 6 July 2020

Keywords:
Pipeline inclination
Oil-water fluid flow
Water accumulation
Numerical modeling

ABSTRACT

In this work, numerical models were developed to investigate the critical inclination of a pipeline to eliminate the water accumulation at the floor of the pipe carrying oil-water fluid. Computational fluid dynamics software was used to establish a geometric model of the pipe with various inclination angles, and a grid-independent verification was conducted to determine a reasonable meshing method. Quantitative relationships were determined between the pipe inclination angle and the affecting factors including the flow velocity, viscosity and the pipe diameter, where the water accumulation would not be able to occur. Generally, the critical inclination angle increases with the fluid flow velocity. The refluxing of water is the key mechanism causing the water accumulation at the bottom of the pipe. In addition to the fluid flow velocity, an increase in fluid viscosity and a decrease in the pipe diameter cause an increase of the critical inclination angle that the water phase can be carried away by oil. The model can be used to determine the critical inclination of pipelines carrying oil-water fluid to cause the water accumulation and the operating conditions that can eliminate the accumulation of water phase at the pipe floor.

1. Introduction

In the pipeline transportation process of crude oil, due to the influence of pipeline elevation, terrain relief and oil-water density difference, there is often water accumulation in low-lying pipeline, as shown in Fig. 1. Water acts as an electrolyte solution in the process of corroding galvanic cells [1], which will accelerate electrochemical corrosion [2]. By analyzing the flow of water-containing crude oil in the pipeline and focusing on the detection of the location where water may be generated in the pipeline, the hidden safety of the pipeline can be solved to a large extent [3].

As the research results shown in Table 1, a large number of scholars have conducted experimental studies on oil-water two-phase flow under different working conditions. Due to the limitation of the experimental conditions [4], the diameter of the experimental tube at this stage is difficult to exceed 50.8 mm, and the experimental medium is mainly easy-to-observe refined oil and mineral oil. The main observation data are flow pattern, phase distribution, pressure drop and liquid holding rate. However, there are few studies on the critical dip angle of oil-carrying water under different working conditions.

Oil-water two-phase flow has the characteristics of unstable flow, many changes in flow pattern, large flow resistance, and complex interphase. The critical inclination of oil-carrying water is greatly affected by pipeline parameters and fluid properties [5]. However, due to the limitation of experimental conditions, the diameter and inclination range of the pipeline are relatively small

* Correesponding author.
E-mail address: 201821000753@stu.swpu.edu.cn (D. Li).
Peer review under responsibility of Southwest Petroleum University.

Production and Hosting by Elsevier on behalf of KeAi

https://doi.org/10.1016/j.petlm.2020.07.001

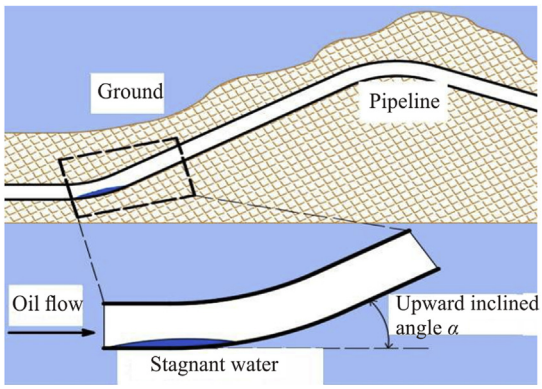

Fig. 1. Schematic diagram of the accumulation of stagnant water in a pipeline at some inclinations.

in the investigation experiment; and mineral oil is widely used in the oil-water two-phase flow experiment, without considering the influence of the change range of crude oil viscosity. Therefore, it is of great significance to study the critical operating conditions of oil-water two-phase flow for crude oil to take away the water accumulated at the bottom of inclined pipes.

In this paper, the mathematical model of critical angle of oil carrying water is established by numerical simulation, and the applicability of the model is verified by experimental results. Firstly, based on the field conditions, ICEM-CFD software is used to build the pipeline models under different conditions [6]. Then the numerical simulation of crude oil water two-phase flow under different flow rate, viscosity and pipe diameter was carried out by FLUENT software. The Origin software is used to fit the mathematical model of critical inclination angle of crude oil carrying water. Finally, through the oil-water two-phase flow experiment, the crude oil water carrying parameters were obtained to verify the accuracy of the mathematical model.

2. Numerical simulation

The oil-water fluid flow was simulated by a CFD solver (FLUENT 16.0), where the volume of fluid (VOF) model was used [14]. The VOF model is a surface tracking method that can be used to study the liquid-liquid two-phase flow in pipes [15]. Due to the density difference and immiscibility between oil and water, an interface exists between them, and the VOF model can track the volume fraction of each phase in the fluid. In this work, the fluid flow was considered as turbulent [16]. In the VOF model, the mass transfer between phases is ignored, and the governing equations include mass equations, momentum equations, and volume fraction transport equations.

Table 2
Physical properties of the simulated fluid at 20 °C and 1 atm.

Property	Oil	Water
Density (kg/m^3)	843.5	998.5
Viscosity (m Pa ·s)	9.581	1.030

The mass conservation equation is as follows:

$$\frac{\partial \rho}{\partial t} + \nabla \cdot \left(\rho \vec{U}\right) = 0 \tag{1}$$

The momentum conservation equation is as follows:

$$\frac{\partial \left(\rho \vec{U}\right)}{\partial t} + \nabla \cdot \left(\rho \vec{U}\vec{U}\right) = -\nabla p + \nabla \cdot \left[\mu\left(\nabla \vec{U} + \nabla \vec{U}^{\mathrm{T}}\right)\right] + \rho \vec{g} \sin \alpha + \vec{F}_{\mathrm{SF}} \tag{2}$$

The volume fraction transport equation is as follows:

$$\frac{D\beta k}{Dt} = \left(\frac{\partial}{\partial t} + \vec{U} \cdot \nabla\right)\beta k = 0 \tag{3}$$

The oil-water interfacial tension causes a sudden pressure change between phases. The gradient of the sudden change is equal to the increased volume force ($\vec{F}_{SF}$), which is expressed as the source term of the momentum equation.

$$\vec{F}_{SF} = 2\beta k \sigma \kappa \vec{n} \tag{4}$$

The surface normal vector ($\vec{n}$) is defined as the gradient of the volume fraction of a phase:

$$\vec{n} = \nabla \cdot \beta k \tag{5}$$

As the influence of temperature on the fluid flow was mainly indirect by changing the dynamic viscosity of the fluid, the

Table 1
A mini-summary of previous work conducted to investigate fluid flow of oil–water systems.

Work	Pipe diameter (mm)	Pipe inclination (degree)	Fluids	Superficial velocity of water (m/s)	Superficial velocity of oil (m/s)	Research objectives
(Lovick and Angeli, 2004) [7]	38.1	0	–	0.8 to 3.0	0.08 to 2.7	Pressure loss, Phase distribution, water holdup, flow pattern
(Grassi et al., 2008) [8]	21	0, ±15	–	0.1 to 2.5	0.2 to 0.7	Pressure loss, water holdup, flow pattern
(Lum et al., 2006) [9]	38	±5, ±10	Mineral oil	0.7 to 2.5	0.7 to 2.5	Pressure loss, water holdup, flow pattern
(Poesio et al., 2009) [10]	20.3	0	Heavy oil	0.1 to 2.6	0.03 to 0.7	Pressure loss, flow pattern
(Wang et al., 2011) [11]	25.4	0	Heavy oil	0.1 to 1.2	0.1 to 1.2	Pressure loss, flow pattern
(Al-Wahaibi et al., 2012) [12]	25.4/19	0	Mineral oil	0.1 to 0.4	0.06 to 0.29	
(Flores et al., 1999) [13]	50.8	90	Mineral oil	0.05 to 1.3	0.05 to 1.3	Pressure loss, flow pattern

Table 3
Solution method of simulation.

Multiphase flow model		VOF model
Solver		Pressure based solver
Solver algorithm		PISO
Turbulence model		Standard k-ε model
Time step		0.005 s
Maximum number of iterations		50
Boundary Condition	Entrance	Speed entrance
	Outlet	Pressure outlet
Spatial Discrete Method	Gradient	Least Square Cell Based
	Pressure	Body Force Weighted
	Momentum	Second Order Upwind
	Volume fraction	Geo-Reconstruct
	Turbulent Kinetic Energy	Second Order Upwind
	Turbulent Dissipation Rate	Second Order Upwind

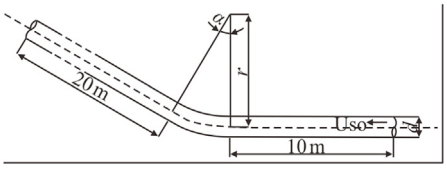

Fig. 2. Schematic diagram of the geometry of pipe to be modeled.

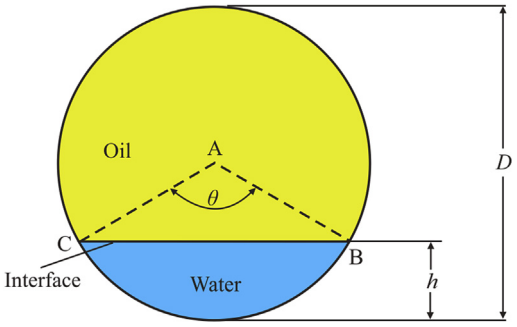

Fig. 3. Schematic diagram of the initial state of the modeled oil-water fluid.

influence of temperature fluctuation on the flow was not considered. A continuous surface tension model was used to transform the surface tension into the source term for the momentum equation. A closed set of equations was formed by building a k-epsilon (k-ε) equation to solve the oil-water flow problem.

2.1. Solution method of simulation

The physical properties of the simulated fluid were set constant, as listed in Table 2. During the simulation, a pressure implicit with the splitting of operators (PISO) algorithm was used, where the combination of the pressure-based method with the implicit physical force method was effective in transient problem

Table 4
Thickness of the first grid near the wall (d = 261.8 mm as an example).

Pipe inner diameter (mm)	Velocity (m/s)	Thickness of the first grid near the wall (mm)
261.8	0.5	10.3186
	0.8	6.8380
	1.0	5.6243
	1.2	4.7923
	1.5	3.9378

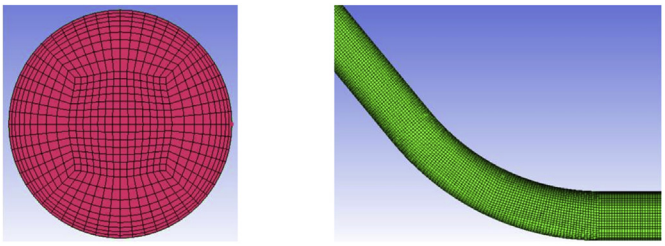

Fig. 4. Grid generation in the model: cross-sectional view (left), and the inclined pipe (right).

Table 5
Meshing strategies developed in the model.

Mesh scheme number	Number of elements
No. 1	505,416
No. 2	1,013,548
No. 3	1,507,072
No. 4	2,038,853
No. 5	2,508,807
No. 6	3,007,628

calculation. The spatial discretization included gradient, pressure, momentum, volume fraction, turbulent kinetic energy and turbulent dissipation rate. By referring to the experience of numerical simulation of oil-water two-phase flow and analyzing the convergence and stability of various models and simulation methods, the models and methods of the simulation process in this paper are screened. The results are shown in Table 3. It was assumed that the height of the initial water phase was constant. The convergence of the calculation results was evaluated by calculating the residuals. When the ratio of the absolute residual of variables decreased by six orders of magnitude and the difference in net mass flows between the inlet and the outlet was less than 10^{-5}, the simulation results were considered convergent [17].

2.2. Pipe geometry to be modeled

A 3-dimensional pipe model was developed using ANSYS ICEM CFD software to simulate the oil-water flow, as shown in Fig. 2. The horizontal part of the pipe was 10 m long. The upward part of the pipe was 20 m long, with a curvature radius of 5*D*, where *D* was outer diameter of the pipe. The internal diameters modeled were 261.8 mm, 495.2 mm, 644.2 mm and 794 mm. The inclination angle

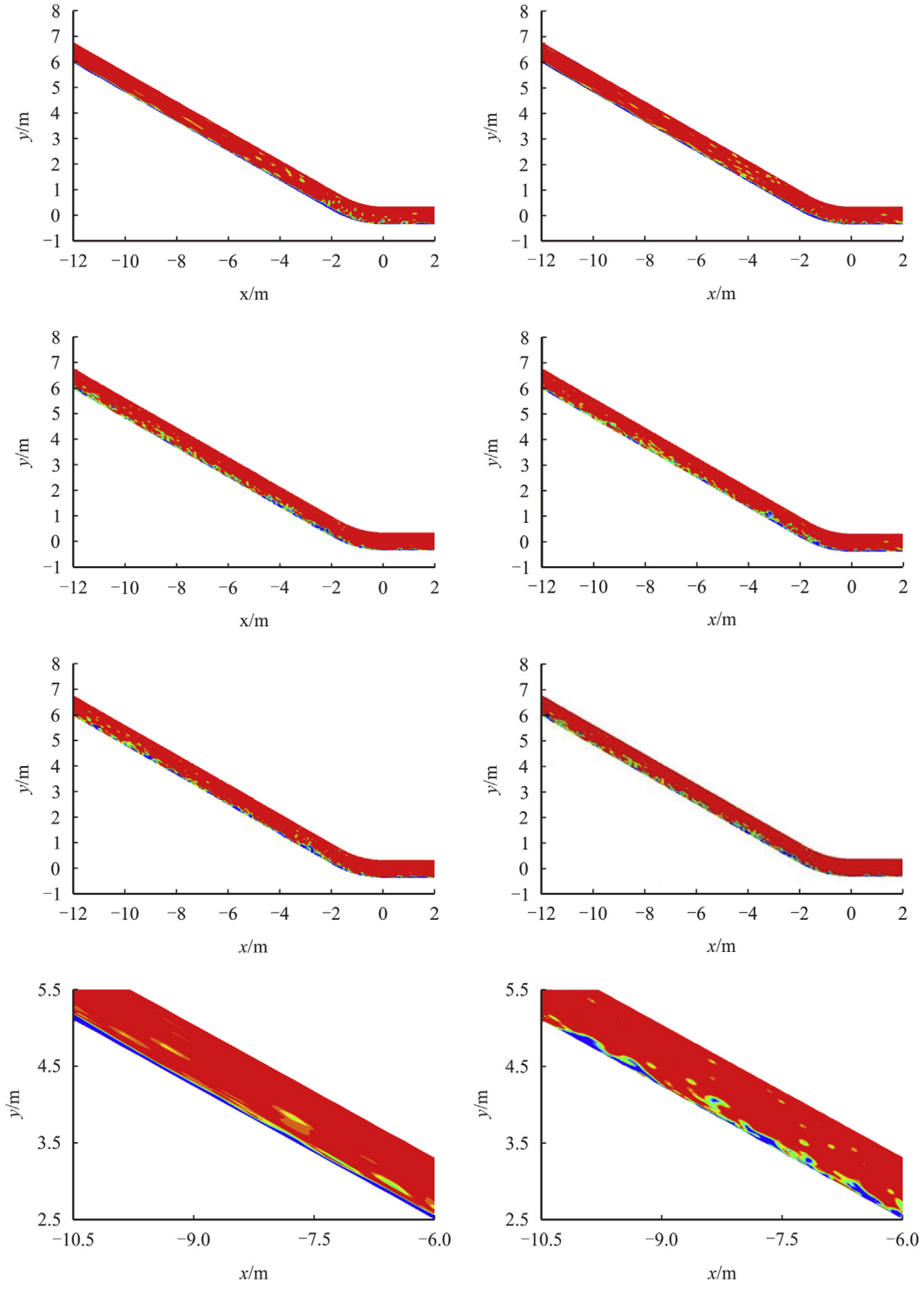

Fig. 5. Simulation results of the mesh schemes, and the detailed view of No. 2 and 3 schemes.

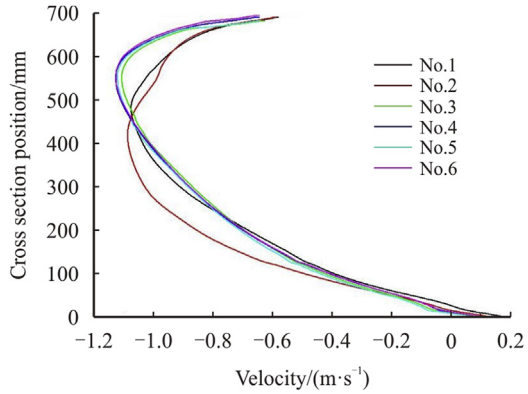

Fig. 6. Distribution of velocity along the center of the pipe at the cross section of x = 10 m.

Table 6
Grid number selection for pipes with varied diameters.

External diameter (mm)	Total number of grids (×10,000)
273	100
508	150
660	150
711	150
813	200

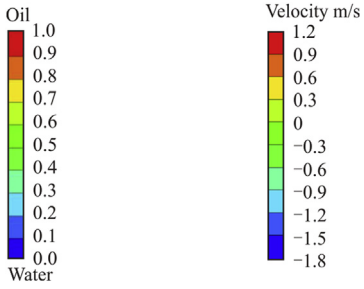

Fig. 7. Oil water distribution legend (left); speed distribution legend (right).

was up to 50°, with 5° of the increment. Assume that the initial water level in the pipe was constant, and determined by the initial water volume, as shown in Fig. 3.

2.3. Boundary conditions

There are three boundaries for oil pipelines, i.e., entrance, exit and pipe wall. A velocity entrance was adopted at the entrance boundary, and the input velocity was the apparent velocity of the oil phase. At the outlet, a pressure condition was used to prevent reverse flow of the fluid. The gradient of the normal velocity was large at the pipe wall. For flow calculation in this area, it was assumed that the fluid was in a stagnant state on the pipe wall, and the standard wall function method was used for the wall boundary [18]. The resolution of the mesh is controlled by Y+, and its function is to calculate the node position of the first layer in the process of mesh generation. In most calculations, the value of Y+ is set between 30 and 300 [19].

According to the online Y+ calculator provided by NASA, the thickness of the first layer grid near the wall of the pipeline under different flow conditions is calculated, as shown in Table 4. The thickness of the remaining layer grid near the pipe wall increases with a scale factor of 1.1. The surface roughness of the pipe wall shall be determined according to the experience of ordinary steel pipe ($\delta = 0.0318$ mm).

2.4. Meshing method analysis

An ICEM CFD software was used to mesh the model of oil-water fluid in the inclined pipeline, where the O-Block method was taken to construct the grids, as shown in Fig. 4. It is seen that the grid is regular and evenly distributed, with a high quality of the boundary layer division and a low probability of element distortion.

To accurately determine the fluid flow condition in the pipe, a grid independent study was performed to obtain sufficient grid density [20]. Six types of mesh scheme were investigated, as shown in Table 5, in the model ($D = 711$ mm, $\alpha = 30°$, $U_{so} = 0.8$ m/s, $\nu_o = 12$ mm^2/s), and the simulation results are shown in Fig. 5. When the number of grids is low (0.5 and 1 million), the water phase diagram in the updip section is distorted, and the oil-water fluctuation interface is obviously different from the result of the large number of grids, which is caused by the low quality of grids.

In order to determine the reasonable number of grids, the flow velocity distribution in the tube with different number of grids in Fig. 5 is analyzed. If there is no obvious difference in the velocity distribution of the fluid, it is considered that the results obtained by using the sparse grid are acceptable. Fig. 6 shows the velocity distribution along the center of the pipe (z = 0) on the x = 10 m cross section. It can be seen from Fig. 6 that the simulation results of No.1 and No.2 deviate greatly from the higher quality mesh generation results. Since No.3, the velocity distribution results have nothing to do with the mesh generation density. For the mesh containing 1.5 million elements (No. 3), the simulation result was almost consistent with that of the 3-million mesh (No.6). The simulation results show that No.3, No.4, No.5 and No.6 are basically the same in terms of oil-water distribution cloud chart and section velocity distribution, and it can be considered that the calculation result grid is irrelevant. As No.3 meshing contained relatively fewer grids with saved computational time, No. 3 (1.5-million mesh) was selected for the simulation analysis of oil–water flow in this model.

The grid independent validation method for other diameters was similar, and the results are shown in Table 6.

3. Modeling results

3.1. Effect of flow velocity

In order to facilitate the comparison of simulation results under different working conditions, all simulation cloud charts use the same oil-water distribution proportion and velocity distribution proportion, in which blue (volume fraction 0) represents water and red (volume fraction 1) represents oil, as shown in Fig. 7.

The superficial velocity of the oil phase was numerically modeled with other variables including viscosity (12 mm^2/s), pipe diameter (711 mm), pipe wall thickness (9.5 mm) and the ratio of oil-water volume (5%) fixed. Fig. 8 shows the simulation results of oil-water two-phase under the condition of fluid velocity of 0.8 m/s, and the velocity distribution cloud chart of the fluid in the pipe when the inclination angle of the pipe is 15°。 It is noted that, as the positive direction of *x* axis is set as positive, the flow direction of the fluid in the pipe is negative. It is seen that the oil–water fluid flow follows a typical wavy pattern. The flow velocity of the upper part of the updip pipe is −0.8 m/s, which is consistent with the inlet flow rate. Positive flow rates, as marked in yellow and red, are identified at the lower part of the pipe, indicating a backflow at the bottom of the pipe. The accumulated water can be completely carried out of the elbow by oil when the inclination is less than 15° only.

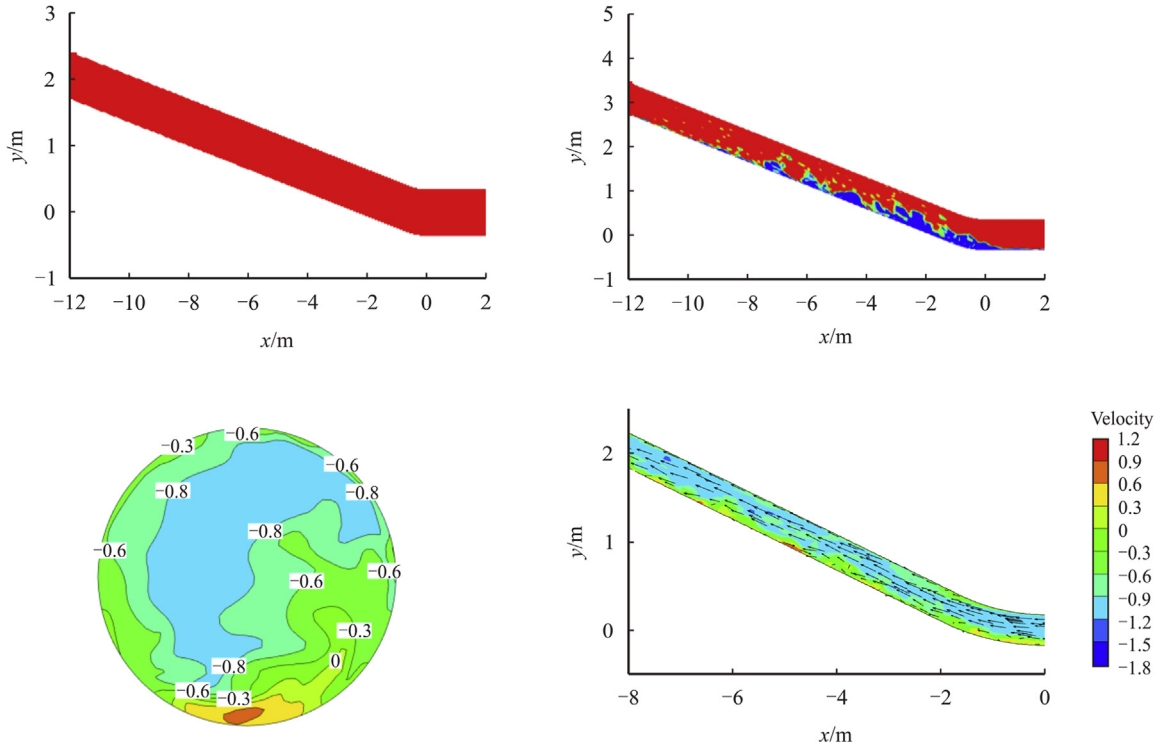

Fig. 8. The simulation results of 10° and 15° pipe inclination at 0.8 m/s and the flow velocity distribution in the pipe with 15° inclination.

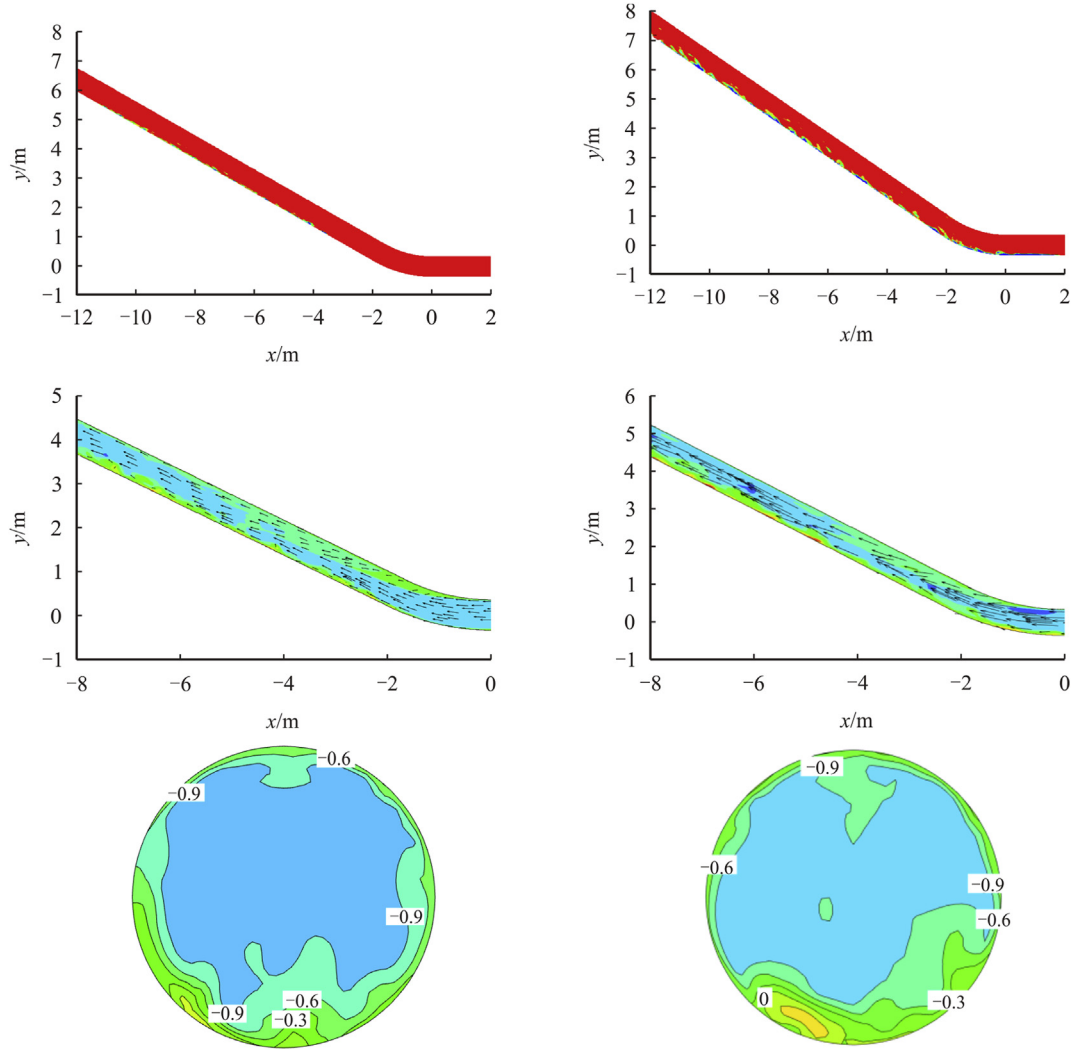

Fig. 9. The simulation results of 30° and 35° pipe inclination at 1.0 m/s flow rate and the corresponding flow velocity distribution in the pipe.

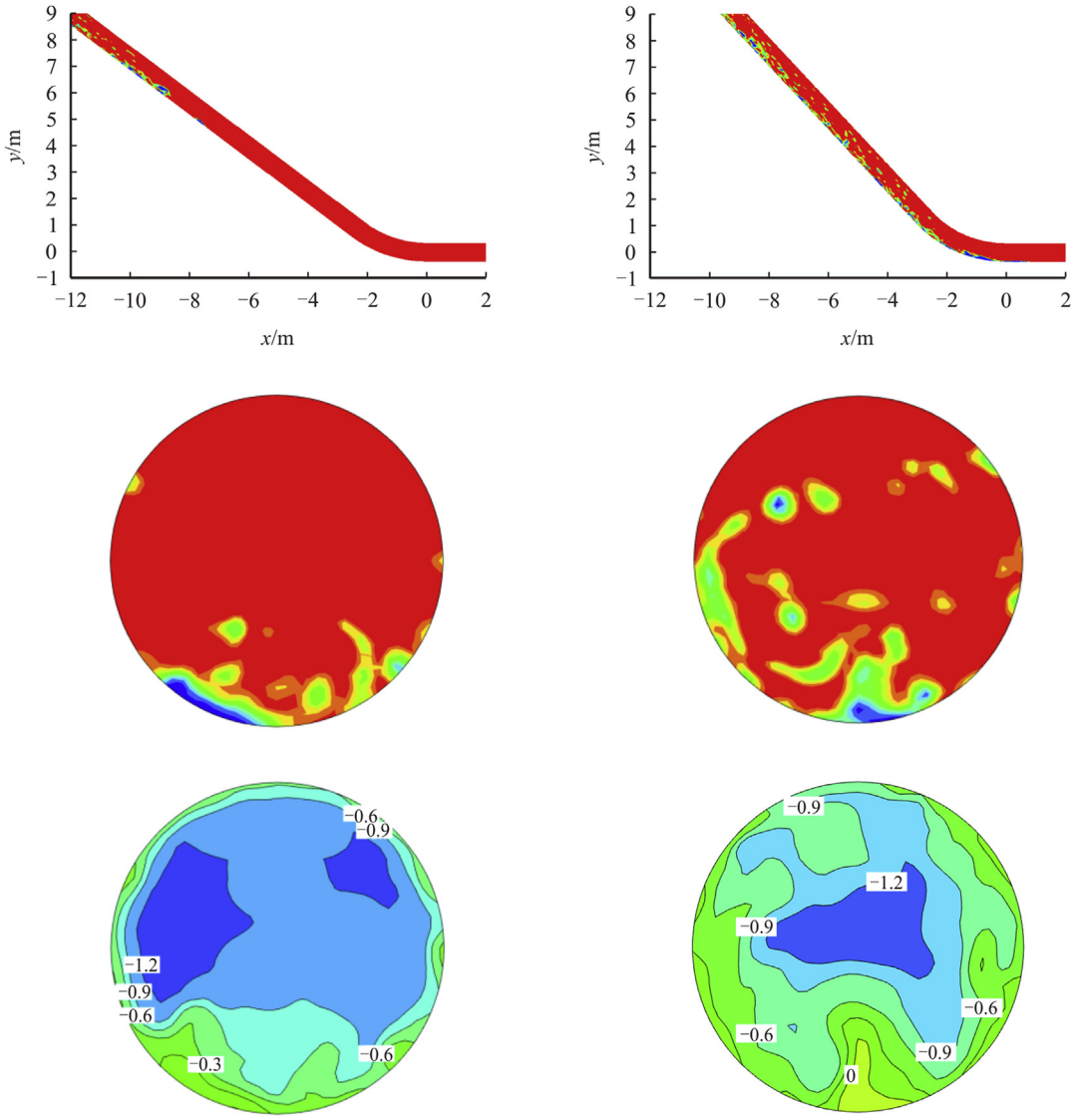

Fig. 10. Modeling of the oil-water fluid flow at the center line (i.e., $z = 0$) at the flow velocity of 1.2 m/s and the inclination angles 45° of and 50°, respectively, and the associated phase and velocity profiles.

Fig. 9 shows the simulation results of inclination angles of 10° and 15° under the condition of a flow velocity of 1.0 m/s, and the corresponding velocity distribution clouds. With the increased flow velocity, the accumulated water is carried out of the pipe with an inclination angle up to 30°. There is no reflow observed.

When the inclination angle is 35°, the fluid in the lower wall of the pipe shows a positive velocity, and the accumulated water is recirculated. Thus, the water phase is not completely emptied. When the flow velocity is increased 1.2 m/s, the oil-water fluid flow is modeled, and the relevant results are shown in Fig. 10. When the pipe inclination angle is 45°, water accumulated in the pipe can be completely carried away by oil. However, the water phase velocity in the bottom of the pipe with an inclination of 50° is positive, indicating that the water phase is recirculated under this condition, resulting in the water accumulation in the pipe that is not carried by oil.

Fig. 11 shows the simulation results under the conditions of 1.5 m/s flow rate and the velocity distribution diagram with an inclination angle of 50°.With the further increased flow rate, all the accumulated water is carried away by oil. There is no water phase remaining in the pipe, indicating that the water phase is carried by the oil phase at the flow rate.

Based on the modeling results, the relationship between the flow velocity of the oil-water fluid and the critical inclination angle under the given condition, i.e., viscosity of 12 mm^2/s, pipe diameter of 711 mm, pipe wall thickness of 9.5 mm and the ratio of oil-water volume of 5%, is determined, as shown in Table 7. Clearly, as the fluid flow velocity increases, the water phase accumulated in the pipe is easy to be carried away, resulting in an increasing critical inclination angle. Moreover, the velocity profile maps show that the reflux is the root cause of the water accumulation in the pipe. When the fluid in the low portion of the pipe is subject to a positive flow rate due to gravity, wall friction or energy loss caused by the vortex inside the pipe, the water phase in the pipe cannot be completely carried away by the fluid flow.

3.2. *Effect of pipe diameter*

Similarly, numerical modeling was conducted on the oil-water fluid flow in the pipe with varied diameters while other

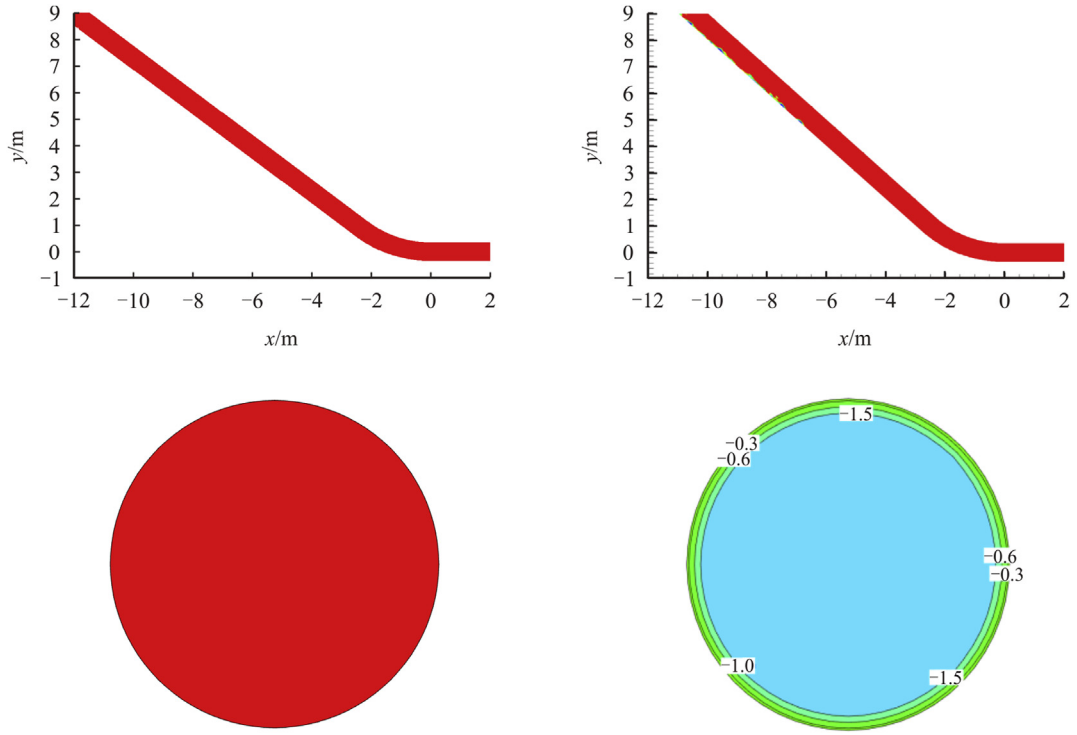

Fig. 11. Modeling of the oil-water fluid flow at the center line (i.e., $z = 0$) at the flow velocity of 1.5 m/s and the inclination angles 45° of and 50°, respectively, and the associated phase and velocity profiles at 50°.

Table 7
Relationship between the flow velocity of the oil-water fluid and the critical inclination angle under the given condition, i.e., viscosity of 12 mm^2/s, pipe diameter of 711 mm, pipe wall thickness of 9.5 mm and the ratio of oil-water volume of 5%.

U_{so} (m/s)	Critical inclined angle (deg)
0.8	10
1.0	30
1.2	45
1.5	>50

conditions such as viscosity (12 mm^2/s), flow velocity (1.0 m/s) and the ratio of oil-water volume (5%) are fixed. The critical inclination angle of the pipe was then determined by analyzing the phase and velocity profiles. Fig. 12 shows the modeling results of the oil–water fluid flow at the center line of the pipe with a diameter of 660 mm at the inclination angles of 35° and 40°, and the velocity profile at the inclination of 40°. It is seen that accumulated water can be carried out at 35°. At the inclination of 40°, water phase remains at the cross section of the pipe and the fluid flow rate is positive, indicating that the water phase in the pipe cannot be fully carried away at the flow rate of 1.0 m/s.

Table 8 shows the relationship between the pipe diameter and the critical inclination angle under the given condition, i.e., viscosity 12 mm^2/s, flow velocity 1.0 m/s and the ratio of oil-water volume of 5%. It is seen that the increase in the pipe diameter favors accumulation of water in the pipe. As a result, the critical inclination of the pipe decreases. The reason is that, while the viscosity and velocity of the fluid are constant, the Reynolds number of the fluid increases as the diameter of the pipe increases. The fluid flow tends to be turbulent. The vortex and backflow at the wall of the pipe increases the energy loss of the water phase, and eventually the recirculation occurs.

3.3. Effect of viscosity

Numerical modeling was conducted on the oil-water fluid flow with varied oil viscosities while other conditions such as flow velocity (1.0 m/s), pipe diameter (711 mm) and the ratio of oil-water volume (5%) are fixed. The critical inclination angle as a function of the kinematic viscosity was determined by analyzing the phase and velocity profiles of the pipe fluid. Fig. 13 shows the results of the oil–water fluid flow at the center line of the pipe with a viscosity of 10 mm^2/s at the inclination angles of 30° and 35°, and velocity profiles at the inclination of 35°. It is seen that there are positive velocities in the low part of the pipe, indicating the recirculation of water phase. Thus, water cannot be completely discharged at the condition.

Table 9 shows the relationship between the viscosity and the critical inclination angle under the given condition, i.e., flow velocity 1.0 m/s, pipe diameter 711 mm and the ratio of oil-water volume of 5%. Since the shear stress is proportional to the viscosity, the shearing action of oil relative to the aqueous phase would increase with the increased viscosity. The accumulated water is expected to be carried away from the pipe. Thus, the critical inclination angle increases.

4. Result and discussion

4.1. Computational modeling for critical inclination of pipelines

Fig. 14 shows the schematic diagram of the modeled oil-water fluid flow in an inclined pipe. The control volume (CV) is selected as the research object. The dimensionless Eötvös number (*Eo*) is calculated by Eq. (6) [21].

$$Eo = \frac{4\pi^2\sigma}{\Delta\rho g d^2} \tag{6}$$

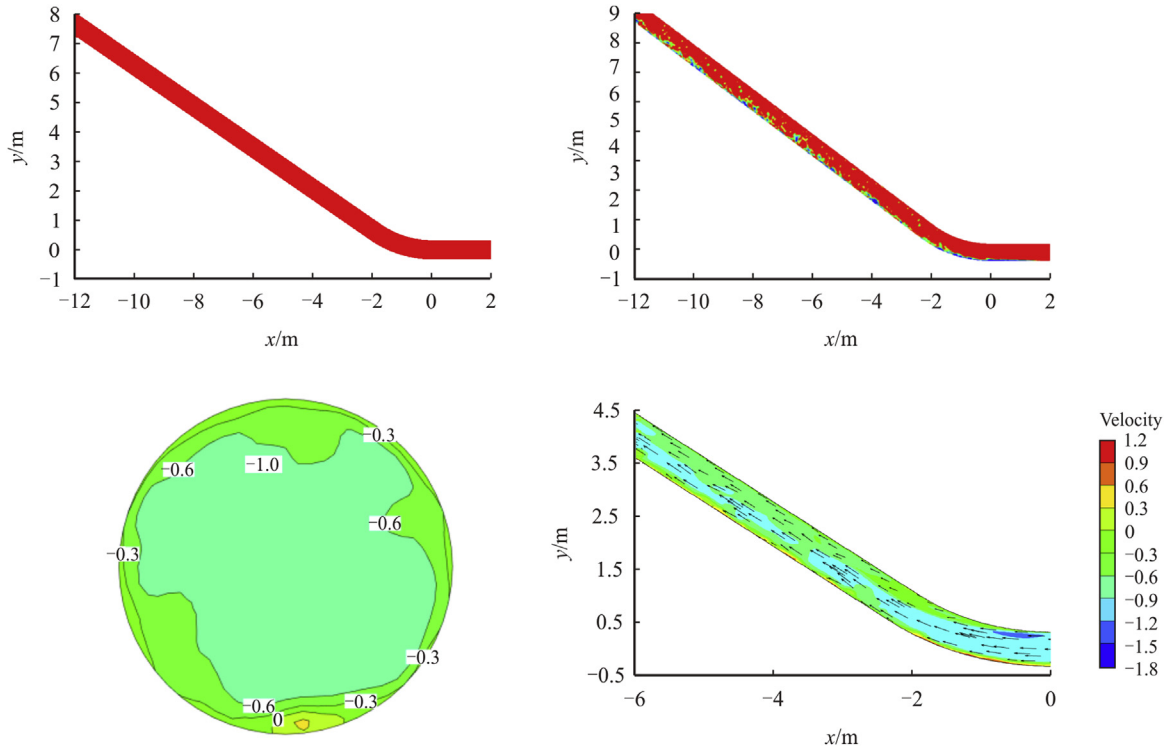

Fig. 12. Modeling results of the oil–water fluid flow at the center line of the pipe with a diameter of 660 mm at the inclination angles of 35° and 40°, respectively, and the velocity profile at the inclination of 40°.

For the conditions with $Eo < 1$, the gravity dominates, and the Froude number similarity criterion is used. However, the similarity between the model and the prototype would be poor if only the Froude number similarity criterion was used. For the liquid–liquid binary phased fluid flow in the pipe, the fluid motion is affected by pressure, viscous forces and surface tension. The critical inclination should be affected by multiple factors including flow velocity, gravity, viscous forces, pressure and surface tension. Eq. [7] is the relation between the critical inclination, α_c, of oil-water flow and the relevant affecting factors:

$$\sin \alpha_c = F(U, d, \Delta\rho, \mu, \sigma, \Delta p) \tag{7}$$

The critical state of the CV is the one that the water phase is carried by oil out of the inclined pipe section so that the water accumulation does not occur. Under the critical condition, the Reynolds number of the oil phase in the controlled volume is calculated by:

$$Re_o = \frac{\rho_o U_o d}{\mu_o} \tag{8}$$

The Froude number of the oil phase in the CV is calculated by:

$$Fr_o = \frac{{U_o}^2}{gd}\cos\alpha \tag{9}$$

The Weber number of the fluid in the CV is approximated as:

$$We = \frac{\rho l U^2}{\sigma} = \frac{\rho_0 d U_o^2}{\Phi\sigma_0} \tag{10}$$

Let $We' = \frac{\rho_0 l U_o^2}{\sigma_0}$, where Φ is the equation for calculating the surface tension of the oil–water flow, and σ_0 is the unit surface tension.

The pressure drop between the two sections 1-1 and 2-2 in the CV is solved by the Bernoulli equation. The Euler number of the oil phase in the CV is calculated by:

$$Eu_o = \frac{\Delta p}{\rho_o U_o^2} \tag{11}$$

Eq. [12] is obtained by passing a series of operations on Eq. [7] based on the π theorem:

$$\sin \alpha_c = F(Re_o, Fr_o, We, Eu_o) = F\left(Re_o, Fr_o, \frac{1}{\Phi}We', Eu_o\right) \tag{12}$$

Based on the numerical modeling results, the oil-water flow in the pipe with an inclination angle less than 50° is discussed herein. A 5° gradient range is adequate for the operating conditions of the pipeline. According to the similarity criteria, the critical inclination angle computational model is fitted by Origin based on the modeling results, as shown in Fig. 15, where the critical inclination angle of the pipe carrying the oil-water fluid can be calculated by:

$$\sin \alpha_c = 0.737 \frac{{Fr_o}^{0.624} {We'}^{0.524}}{{Re_o}^{0.521} {Eu_o}^{0.109}} \tag{13}$$

4.2. Model validation

Conducting a light crude oil-water two-phase flow experimental study through a large loop [22]. The loop experimental device is 10 m long and 3 m wide. The experimental device consists of oil storage tank [1], gate valve [2,7,10,11,14], centrifugal pump [3], pressure indicator [4], globe valve [5], turbine flow meter [6], injection valve [8], drain valve [9], acrylic blend [12], adjustable hoist frame [13,15] and rubber hose [16]. A schematic diagram of the loop

Table 8
Relationship between the flow velocity of the oil-water fluid and the critical inclination angle under the given condition, i.e., viscosity 12 mm^2/s, flow velocity 1.0 m/s and the ratio of oil-water volume of 5%.

D (mm)	Critical inclined angle (deg)
273	>50
508	45
660	35
813	25

Table 9
Relationship between the viscosity and the critical inclination angle under the given condition, i.e., flow velocity 1.0 m/s, pipe diameter 711 mm and the ratio of oil-water volume of 5%.

ν_o (mm^2/s)	Critical inclined angle (deg)
8	25
10	30
15	40
20	40

experimental apparatus is shown in Fig. 16. The experimental apparatus includes the following five parts:

4.2.1. Oil storage system

The oil storage tank [1] is a cylindrical steel drum with a diameter of 323.9 mm and a height of 1200 mm. The fluid in the tube flows through the rubber hose [16] into the tank. A drain valve is provided at the bottom of the oil storage tank to discharge the sediment at the bottom of the tank.

4.2.2. Flow control system

The flow control system is composed of gate valve [2], centrifugal pump [3], pressure indicator [4], globe valve [5] and turbine flow meter [6]. The centrifugal pump is used to supply energy to the system, and the turbine flow meter is used to measure the flow of fluid in the tube under different working conditions.

4.2.3. Water injection system

The water injection system consists of a main pipe and a bypass pipe. A gate valve [7,11] is provided before and after the main pipe. The middle of the main pipe is provided with a water injection valve [8] and a drain valve [9]. A gate valve [10] is provided on the bypass pipe to ensure fluid stability during the water injection process and to reduce the impact of the water injection system on the experiment.

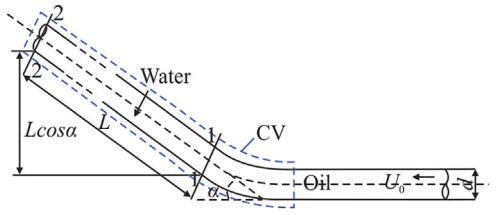

Fig. 14. Schematic diagram of the modeled oil-water fluid flow in an inclined pipe.

4.2.4. Transparent observation section

After the water injection system, the pipe is connected to an acrylic bend [12] of different inclination angles. The diameter of the elbow is Φ 60 × 5, the radius of curvature (r) is 5d (r = 250 mm), the horizontal section and the inclined section are each 1 m long, and the upward tilting angle ranges from 10° to 45° with a gradient of 5° (Total 8 groups).

4.2.5. Support and adjustment system

Adjustable hoist frame support [13,15] for adjusting and fixing a

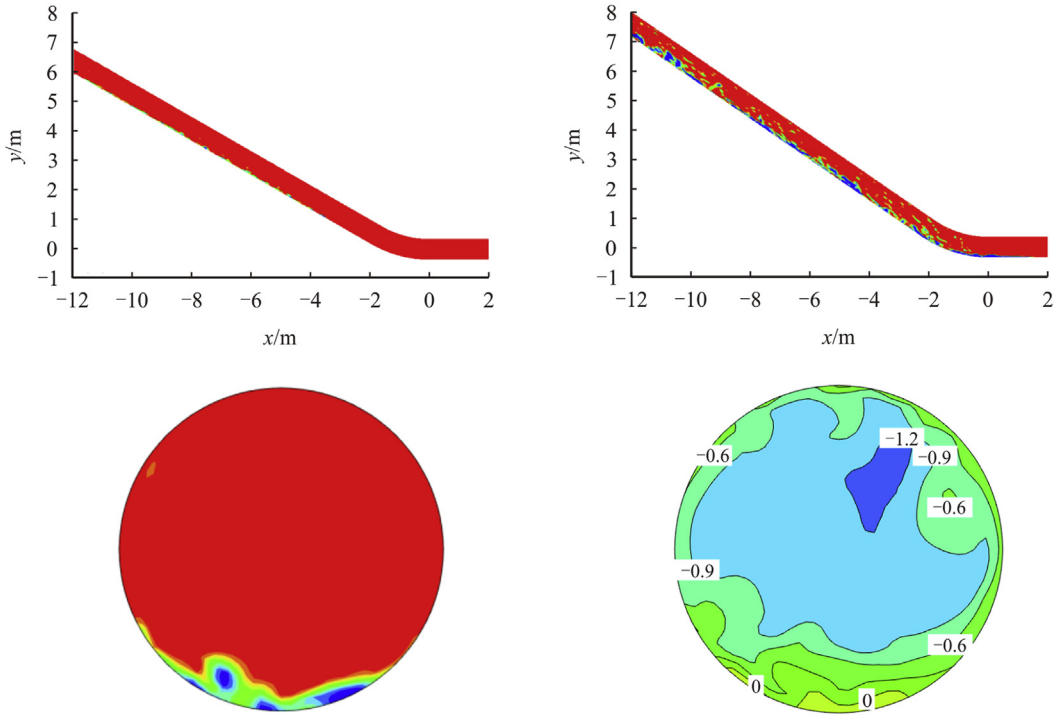

Fig. 13. Modeling results of the oil–water fluid flow at the center line of the pipe with a viscosity of 10 mm^2/s at the inclination angles of 30° and 35°, and velocity profiles at the inclination of 35°.

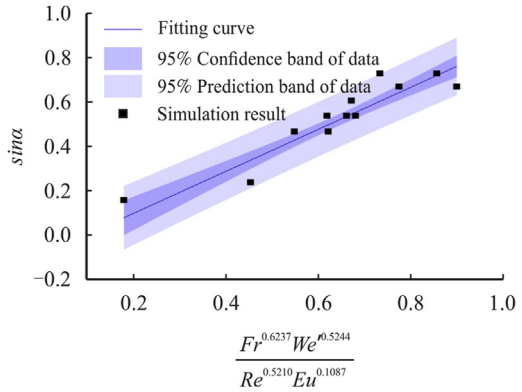

Fig. 15. Critical inclination angle obtained by fitting by Origin based on the modeling results.

transparent observation section, to prevent breakage during the experiment pipe.

The experimental study was carried out under the conditions that both the fluid temperature and the ambient temperature were 20°C and the pressure was a standard atmospheric pressure of 101.325 kPa. Inject 5 L of water from the water injection port and slowly bring the water phase to the acrylic bend at low flow rate with crude oil. Then, the initial flow rate of the crude oil was controlled to be 0.1 m/s, and the oil phase flow rate was gradually increased with a gradient of 0.01 m/s until the water phase in the tube was completely discharged. The physical properties of crude oil and water selected by the experimental research are shown in Table 10. And Table 11 shows the experimental results.

Fig. 17 shows the experimental results and simulation results. As can be seen from Fig. 17, the equation [13] obtained by fitting the simulation results is also applicable to the experimental research results. At the same time, the reliability of the empirical formula of the critical inclination angle of the oil in the updip pipeline and its influencing factors is verified.

4.3. Applicability of the model

(a) The model mainly studies the light crude oil with kinematic viscosity less than 20 mm^2/s. For the crude oil with higher viscosity, the content of colloid and asphaltene is also higher, and the flow state and corrosion in the pipeline are more complex, so further analysis is needed.

(b) In the process of simulation, the principle of dichotomy is used to approach the critical angle of oil carrying water. In the process of simulation, the gradient of pipe inclination is 5°, which will cause deviation to the result. And the inclination angle of the pipeline studied in this paper is not more than 50°.

5. Conclusions

Through numerical simulation and loop experiment, it is found that the backflow of water phase in the updip section is the root cause of water accumulation in the pipe. Based on the principle of dichotomy and the principle of controlling single variable, the numerical simulation of crude oil-water two-phase flow under different flow rates, viscosities and pipe diameters is carried out. It is found that increasing flow rates, viscosities or reducing pipe diameters will lead to the increase of critical inclination. Due to the

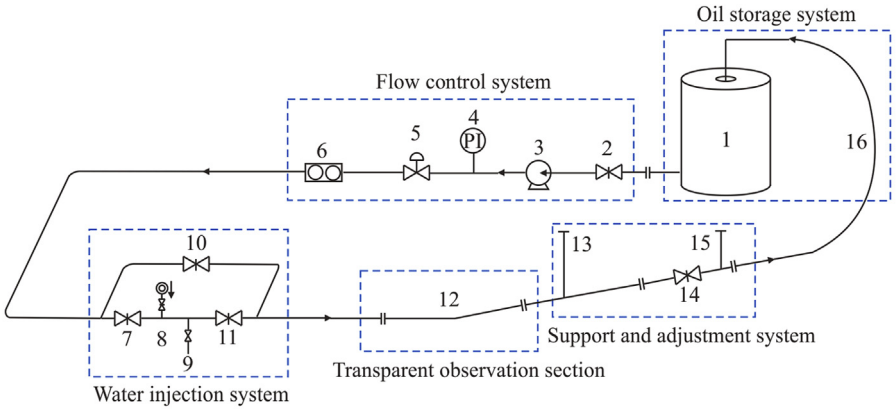

(a)

(b)

Fig. 16. The experimental setup. (a) Schematic description; (b) Picture.

Table 10
Properties of the liquid at 20 °C and 1 atm.

Liquid	Crude oil	Water
Density (kg/m^3)	ρ_o = 843.5	ρ_w=998.5
Viscosity (mPa·s)	μ_o = 9.581	μ_w = 1.030

Table 11
Critical conditions under condition that d = 50 mm, V = 5 L.

Inclined angle (deg)	Critical flow rate (m^3/h)	Critical flow velocity (m/s)
10	1.985	0.281
15	2.254	0.319
20	2.423	0.343
25	2.487	0.352
30	2.755	0.390
35	2.904	0.411
40	3.031	0.429
45	3.123	0.442

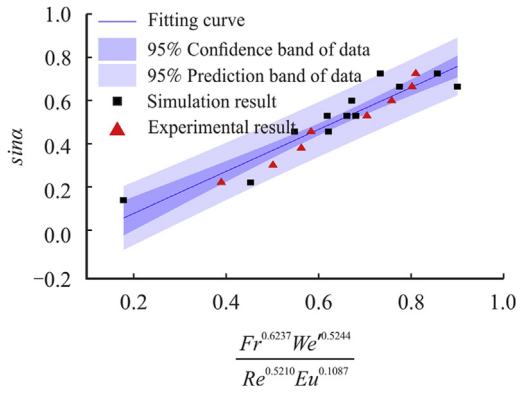

Fig. 17. Validation of the model.

coupling of various factors (such as velocity, viscosity, diameter, etc.), dimensionless quantity is introduced by using π theorem, and the mathematical model of critical inclination angle of crude oil carrying water is fitted by using Origin software. The prediction model has a high accuracy for the critical inclination of light crude oil carrying water. The deviation of the experimental results is smaller and closer to the fitting results.

Declaration of competing interests

The authors declare that they have no conflict of interests.

Nomenclatures

A_o	Oil phase flow area, m^2
A_w	Water phase flow area, m^2
d	Internal diameter of pipeline, mm
D	External diameter of pipeline, mm
Eo	Eötvös number
Eu_o	Euler number of oil phase
Fr_o	Average Froude number
g	Gravitational acceleration, 9.81 m/s^2
V	The volume of water injected in the experiment, m^3
$\vec{F}$	Volume force, N
α	Inclined angle of the pipeline, deg
α_c	Critical inclined angle, deg
Δ	A difference in a physical quantity
μ_o	Average kinematical viscosity of oil, Pa·s
μ_w	Average kinematical viscosity of water, Pa·s
ν_o	Dynamic viscosity of oil, m^2/s
h	Initial thickness of water layer, m
Re_o	Initial thickness of water layer, m
R_{wo}	Ratio of water to oil, %
U_o	Average flow velocity of the oil phase, m/s
U_{so}	Superficial velocity of oil phase, m/s
U	Velocity of the fluid, m/s
We	Average Weber number
l	Length, m
κ	Surface curvature
β_k	Volume fraction of K phase
ν_w	Dynamic viscosity of water, m^2/s
ρ	Density, kg/m^3
ρ_o	Density of oil phase, kg/m^3
ρ_w	Density of water phase, kg/m^3
σ	Surface tension, N/m
σ_0	Unite Surface tension, N/m

Subscript

a	Average value
w	Water phase
o	Oil phase

References

[1] Tao Liu, Y. Frank Cheng, Mohita Sharma, Gerrit Voordouw, Effect of fluid flow on biofilm formation and microbiologically influenced corrosion of pipelines in oilfield produced water, J. Petrol. Sci. Eng. 156 (2017) 451–459, https://doi.org/10.1016/j.petrol.2017.06.026.

[2] G.A. Zhang, Y.F. Cheng, On the fundamentals of electrochemical corrosion of X65 steel in CO_2-containing formation water in the presence of acetic acid in petroleum production, Corrosion Sci. 51 (2009) 87–94, https://doi.org/10.1016/j.corsci.2008.10.013.

[3] H. Hu, Y.F. Cheng, Modeling by computational fluid dynamics simulation of pipeline corrosion in CO_2-containing oil–water two phase flow, J. Petrol. Sci. Eng. 146 (2016) 134–141, https://doi.org/10.1016/j.petrol.2016.04.030.

[4] A.S.I. Ismail, et al., Experimental investigation of oil–water two-phase flow in horizontal pipes: pressure losses, liquid holdup and flow patterns, J. Petrol. Sci. Eng. 127 (2015) 409–420, https://doi.org/10.1016/j.petrol.2015.01.038.

[5] R.C.R.D. Silva, R.S. Mohamed, A.C. Bannwart, Wettability alteration of internal surfaces of pipelines for use in the transportation of heavy oil via core-flow, J. Petrol. Sci. Eng. 51 (2006) 17–25, https://doi.org/10.1016/j.petrol.2005.11.016.

[6] R.G. Walvekar, T.S.Y. Choong, S.A. Hussain, M. Khalid, T.G. Chuah, Numerical study of dispersed oil–water turbulent flow in horizontal tube, J. Petrol. Sci. Eng. 65 (2009) 123–128, https://doi.org/10.1016/j.petrol.2008.12.019.

[7] J. Lovick, P. Angeli, Experimental studies on the dual continuous flow pattern in oil–water flows, Int. J. Multiphas. Flow 30 (2004) 139–157, https://doi.org/10.1016/j.ijmultiphaseflow.2003.11.011.

[8] B. Grassi, D. Strazza, P. Poesio, Experimental validation of theoretical models in two-phase high-viscosity ratio liquid–liquid flows in horizontal and slightly inclined pipes, Int. J. Multiphas. Flow 34 (2008) 950–965, https://doi.org/10.1016/j.ijmultiphaseflow.2008.03.006.

[9] J.Y.L. Lum, T. Al-Wahaibi, P. Angeli, Upward and downward inclination oil–water flows, Int. J. Multiphas. Flow 32 (2006) 413–435, https://doi.org/10.1016/j.ijmultiphaseflow.2006.01.001.

[10] P. Poesio, D. Strazza, G. Sotgia, Very-viscous-oil/water/air flow through horizontal pipes: pressure drop measurement and prediction, Chem. Eng. Sci. 64 (2009) 1136–1142, https://doi.org/10.1016/j.ces.2008.10.061.

[11] W. Wang, J. Gong, P. Angeli, Investigation on heavy crude-water two phase flow and related flow characteristics, Int. J. Multiphas. Flow 37 (2011) 1156–1164, https://doi.org/10.1016/j.ijmultiphaseflow.2011.05.011.

[12] T. Al-Wahaibi, N. Yusuf, Y. Al-Wahaibi, et al., Experimental study on the transition between stratified and non-stratified horizontal oil–water flow, Int. J. Multiphas. Flow 38 (2012) 126–135, https://doi.org/10.1016/j.ijmultiphaseflow.2011.08.007.

[13] J.G. Flores, X.T. Chen, J.P. Brill, Characterization of oil-water flow patterns in vertical and deviated wells, SPE Prod. Facil. 14 (1999) 94–101, https://doi.org/10.2118/56108-PA.

[14] G. Xu, L. Cai, A. Ullmann, N. Brauner, Trapped water flushed by flowing oil in upward-inclined oil pipelines, in: 2012 9th International Pipeline Conference, Am. Soc. Mech. Eng, 2012, pp. 637–647, https://doi.org/10.1115/IPC2012-90680.

[15] M. Mohammadi, S. Shahhosseini, M. Bayat, Direct numerical simulation of

water droplet coalescence in the oil, Int. J. Heat Fluid Flow 36 (2012) 58–71, https://doi.org/10.1016/j.ijheatfluidflow.2012.04.001.
[16] A.B. Desamala, A.K. Dasamahapatra, T.K. Mandal, Oil-water two-phase flow characteristics in horizontal pipeline–a comprehensive CFD study, World Acad. Sci. Eng. Technol. Int. J. Chem. Mol. Nucl. Mater. Metall. Eng. 8 (2014) 360–364.
[17] G. Xu, L. Cai, A. Ullmann, N. Brauner, Experiments and simulation of water displacement from lower sections of oil pipelines, J. Petrol. Sci. Eng. 147 (2016) 829–842, https://doi.org/10.1016/j.petrol.2016.09.049.
[18] M.J. Hancock, J.W.M. Bush, Fluid pipes, J. Fluid Mech. 466 (2002) 285–304, https://doi.org/10.1017/S0022112002001258.
[19] L. Wang, D. Gao, Y. Zhang, Numerical simulation of turbulent flow of hydraulic oil through 90 degrees circular-sectional bend, Chin. J. Mech. Eng. 25 (2012) 905–910, https://doi.org/10.3901/CJME.2012.05.905.
[20] A. Alias, J. Koto, Y.M. Ahmed, CFD simulation for stratified oil-water two-phase flow in a horizontal pipe, in: Proceeding of Ocean, Mechanical and Aerospace-Science and Engineering 1, 2014, pp. 20–25.
[21] N. Brauner, D.M. Maron, Identification of the range of small diameters conduits, regarding two-phase flow pattern transitions, Int. Commun. Heat Mass Tran. 19 (1992) 29–39, https://doi.org/10.1016/0735-1933(92)90061-L.
[22] X. Song, Y. Yang, T. Zhang, K. Xiong, Z. Wang, Studies on water carrying of diesel oil in upward inclined pipes with different inclination angle, J. Petrol. Sci. Eng. 157 (2017) 780–792, https://doi.org/10.1016/j.petrol.2017.07.076.